IL NUOVO CIMENTO Vol. 34 C, N. 4 Luglio-Agosto 2011
DOI 10.1393/ncc/i2011-10914-x

Colloquia: Channeling 2010

# Use of single carbon nanotubes and graphene in particle detectors and beam monitors

K. A. Ispirian(*) and R. K. Ispiryan
*Yerevan Physics Institute - Yerevan, Armenia*

(ricevuto il 22 Dicembre 2010; pubblicato online il 7 Luglio 2011)

**Summary.** — After a short review of some physical properties of single carbon nanotubes and graphene layers it is discussed the possibility of construction of new beam particle monitors (BPM), ionization and proportional counters and time projection chambers (TPC). It is shown that in spite of the tested laser and wire BMPs the proposed single nanotube BPMs can provide better measurement of the profile of future electron-positron colliders with very high beam density. The use of single nanotubes as anode wires in proportional counters allows their operation at lower electric fields and to construct multiwire proportional counters (MPC) with better space resolution. It is proposed to construct TPCs using nanotubes and graphene ribbons based on the sharp variation of graphene electrical conduction under the influence of electrostatic potential resulting from the charge deposited by the ionizing particles.

PACS 61.48.De – Structure of carbon nanotubes, boron nanotubes, and closely related graphitelike systems.
PACS 68.65.Pq – Graphene films.
PACS 29.40.Cs – Gas-filled counters: ionization chambers, proportional, and avalanche counters.

## 1. – Introduction

The carbon nanotubes (NT) discovered in [1] and rediscovered in [2] have found wide application due to their mechanical, heat, electrical and other physical properties. The physical properties of NT nanocrystals allow their use in high energy physics [3-5]. Recently bulky NTs have been used for detection of photons within frequency intervals from radiowaves up to IR [6] and UV [7]. Using single NTs instead of silicon, nanotube field effect transistors (NTFET) have been obtained (see [8]), and works are going to use NTFETs not only for dosimetry, but also for preparing integrated circuits (chips) [9] for

(*) E-mail: karo@mail.yerphi.am

 

dosimetric profiling the beams and also as sensor for single charges [10]. In the NTFET detectors of the type described in [9] the principle of operation of which is similar to that of usual MOSFET, the part of energy of the ionizing particles is deposited in a relatively thick undoped semiconductor (Si) producing charges. Due to the voltage between a gate and NT the produced charges pass a thin insulator ($SiO_2$) and then are detected by the "source" and "drain" ends of a single NT. The charges are collected without any electron multiplication. The idea [11] to use NTs as anode wires in proportional chambers with electron multiplication, giving possibility to 1) have lower voltages and 2) better space resolution, is in the process of realization [12]. The difficulty of using NTFET with multiplication is connected with the fact that in the case of gas filling and nanometer anode, the electric field necessary threshold is obtained on distances $\sim$ nm, which is much smaller than the mean free path equal to a few or tens of $\mu$m of electrons in gases. Due to this fact the avalanche process will be suppressed. The use of heavy gas under pressure or liquid inert gases (LAr or LXe) can save the situation. Let us note that LXe provides also gas amplification of $\sim$ 10–100 for thin anodes. That is why with the help of the code Maxwell 3D/2D only results without any amplification are still obtained in [13].

The graphene (GR) has been first obtained in [14]. Even at room temperatures GR monolayers have [15] low electronic noise, high carrier mobility, ten or more times higher than the carriers in silicon, and resistance sensitivity to the neighboring electric field, especially near the so-called Dirac point. Intrinsic GR is a semimetal or 0-gap semiconductor with electron and hole behavior as 0 mass relativistic particles described by Dirac equations for spin 1/2. The graphene nanoribbons (GRNR) are of 2 types: zigzag or armchair depending on the configuration of the un-bonded edges. The zigzag GRNRs are always metallic, while the armchairs can be either metallic or semiconductor. At present there are a few methods for production of GRNR, in particular, by cutting NTs. Just as the above-described NTFET detectors the proposed [16] detector on the basis of GRFET works again without electron multiplication. To our knowledge, at present there have been published: a) the operation principles and Monte Carlo simulation results [16], b) only preliminary results on the GRFET-based dosimetric detector sensitivity to electrons [17] and X-rays [18] beams.

Since in this work the applications of long single NTs and GRNRs will be considered in connection with ionizing particle detection and beam monitoring, it is reasonable to remind some physical properties of the single wall NT, SWNT(10,10) (see [19]): it has diameter $\sim$ 1.3 nm, density $\sim$ 1.33 g cm$^{-3}$, Young's modulus $\sim$ 1 TPa, maximum tensile strength $\sim$ 30 GPa, electrical resistance, $\sim 10^{-4}\,\Omega$ cm, thermal conductivity $\sim$ 2000 W/m/K and negative coefficients of thermal expansion $\sim 6 \cdot 10^{-6}\,\mathrm{K}^{-1}$. It is reasonable also to consider briefly the processes resulting in energy deposition in NT and GRNR, which differ essentially from those taking place in thicker layers of materials. Still in [20] it has been shown that the distribution of the ionization energy losses in thin layers differs from that predicted by the Landau theory [21] or other models [22]. In the case of very thin layers, when the probability of collision of beam particles with layer's atoms is much less than unity [20], this distribution has discrete peaks at certain energies. Having these losses and the probabilities of absorption of the emitted soft and hard photons as well as of $\delta$-electrons, in principle, one can calculate the energy deposited in the layer as in [23]. However, since GR and NTs present single or few layers of carbon atoms, it is clear that only a negligible fraction of the produced secondary electrons or photons produced by ionizations or excitations are absorbed by the carbon atoms, and the production of structural defects has low probability. To our knowledge, the processes

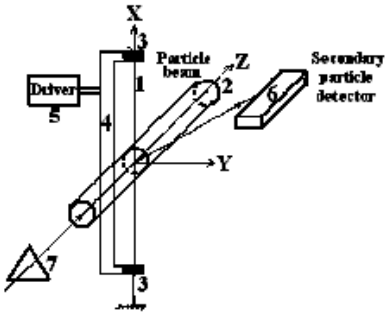


Fig. 1. – A stretched SWNT for BMP: 1) the NT, 2) a particle beam, 3) the clipses, 4) a wire support, 5) a driver, 6) a secondary or scattered particle detector and 7) a steering magnet, respectively.

of energy deposition and of the radiation hardness in NT and GR have not been studied satisfactorily (for a short review see [9]).

Taking into account the above said and the advance in the synthesis of long NT [24], GRNR [25] and nanomanipulation [26], this work is devoted to the possible use of NT and GRNR for particle detection and beam monitoring (part of the results is given in [27]).

## 2. – Beam position monitors (BPM) using NT wires

The horizontal and vertical dispersions, $\sigma_x$ and $\sigma_y$, of the electron beam cross-sections at the interaction points in SLC, SLAC are equal to 1.5 and $0.65\,\mu$m, while in future ILC and CLIC they will be equal to 0.6 and $0.006\,\mu$m and 0.043 and $0.001\,\mu$m, respectively [28, 29]. Thinner wires are required for BMP with better profile resolution. However, as the experiments show, wires with diameters less than $\sim 4\,\mu$m cannot be used since they undergo destructive damages due to thermal energy deposition, if the rms transverse size of $10^9$ electrons is less than $1\,\mu$m [29]. To solve these problems, it has been proposed and tested to replace the solid wire scanner by thin laser beam and to detect the Compton scattered photons [28] or electron-positron pairs [30]. With the help of interference methods the resolution of the recent laser BPM had achieved a few tens of nm [28].

Without discussing the manipulation methods we assume that one has (see fig. 1) a 1-2 cm long SWNT(10,10) conductive wire tidily stretched with the help of two clips on a shifting support, made of material with low coefficient of thermal expansion. The fast scanning of the beam is made with the help of a driver or of the steering magnet detecting the secondary particles with the help of a detector. The particle beam profile can be measured by one of the following methods: 1) Detecting the secondary particles under small angles; 2) Recording the electric current induced in the NT wire due to secondary electron emission as in [31]; or 3) Detecting the $\sim 200$ eV characteristic radiation photons of carbon atoms as in [32]. Considering the rate of the BPM measurements we shall make estimates only for the characteristic radiation method 3). We shall assume that the particle beam bunch has square cross-section $S_{\mathrm{Bunch}} = L_x L_y$ and contains $N_{\mathrm{Bunch}}$ particles with uniform density distribution instead of usual Gaussian distributions. In the case of isolated SWNT target, when the particle beam passes only two atomic layers, and the beam cross-section is larger than the NT transversal sizes, it is reasonable to estimate the number of the produced characteristic quanta in a frame where the beam particles are in

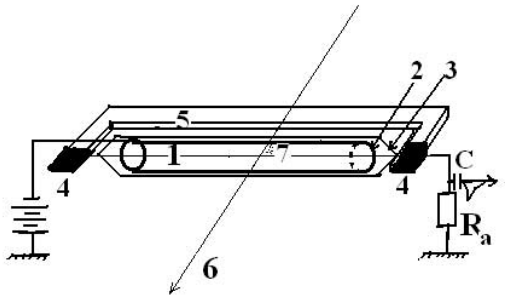


Fig. 2. – A proportional chamber. 1) is a SWNT(10,10), 2) is a cylindrical metallic cathode with $r_c = 5$–$12\,\mathrm{mm}$, 3) is a glass tube containing appropriate gas, 4) are clipses of the NT support 5), and 6) is a particle producing the electron-ion shower 7).

rest using invariance properties of some magnitudes. One can show that the probability of interaction of single target atom with the beam bunch containing $N_{\mathrm{Bunch}}$ particle is equal to $P = n_{Bx}\sigma_{\mathrm{int}}$, where $n_{Bx} = N_{\mathrm{Bunch}}/S_{\mathrm{Bunch}}$ is the surface density of the beam particles "seen" by passing NT atoms, and $\sigma_{\mathrm{int}} = \sigma_K$ is the interaction (in our case the $K$-shell ionization) total cross-section. Therefore, the number of the detected characteristic radiation photons per bunch is equal to $N_{\mathrm{Bunch}}^{\mathrm{Det},K} = FN^{\mathrm{NT}}\Delta\Omega_{\mathrm{Det}}N_{\mathrm{Bunch}}\sigma_K/4\pi S_{\mathrm{Bunch}}$, where $F$ is the target NT atom fluorescence yield, $N^{\mathrm{NT}}$ is the number of atoms of 2 layers of an NT which can interact with the beam cross section, $\Delta\Omega_{\mathrm{Det}}$ is the acceptance solid angle of the detector.

The cross-section of $K$-shell ionization is equal to [33-35]

$$\sigma_K = \sigma_0 \left\{ \frac{1.5}{I} + \frac{0.423}{I} \left[ \ln\left( \frac{1.274}{I}\gamma^2 \right) - 1 \right] \right\}, \tag{1}$$

where $\sigma_0 = 8\pi r_e^2/3 = 0.665 \cdot 10^{-24}\,\mathrm{cm}^2$ and $I = E_K/mc^2$ is the $K$-electron bounding energy in units of electron mass energy. As it follows from (1) the $K$-shell ionization cross-section grows logarithmically with the increase of energy without revealing density effect as in case of ionization energy losses, because harder photons give contribution into $K$-shell ionization. Expression (1) is in good agreement with experimental data [36] up to electron energies 900 MeV, and one can expect it will be correct also in our case at higher energies since the density of the carbon atoms in NT is very low.

In the case of ILC with $L_x = 6 \cdot 10^{-5}\,\mathrm{cm}$, $L_y = 6 \cdot 10^{-7}\,\mathrm{cm}$, $E_e = 500\,\mathrm{GeV}$ or $\gamma = 10^6$, $N_{\mathrm{Bunch}} = 10^{10}$, $n_{\mathrm{Bunch}} = 2.8 \cdot 10^{20}\,\mathrm{cm}^{-2}$, for NT SWNT(10,10) with $I = 4 \cdot 10^{-4}$, $N^{\mathrm{NT}} = 600$, fluorescence yield $F = 0.002$, $\sigma_K = 2.6 \cdot 10^{-20}\,\mathrm{cm}^2$ and for $\Delta\Omega_{\mathrm{Det}} = 10^{-2}\,\mathrm{rad}$ one obtains $N_{\mathrm{Bunch}}^{\mathrm{Det},K} = 6.7 \cdot 10^{-3}$. Taking into account that for ILC the number of bunches per second is $\sim 1.25 \times 10^4$ one obtains that about 80 characteristic photons per second will be detected for the above parameters from a NT BPM on ILC. Such a quantity of characteristic photons is enough to carry out the measurement of the beam profile in short times.

## 3. – Proportional counters using NT wires

Now let us consider the construction and principle of operation of a proportional counter with NT anode schematically shown in fig. 2. In ionization counters the anode

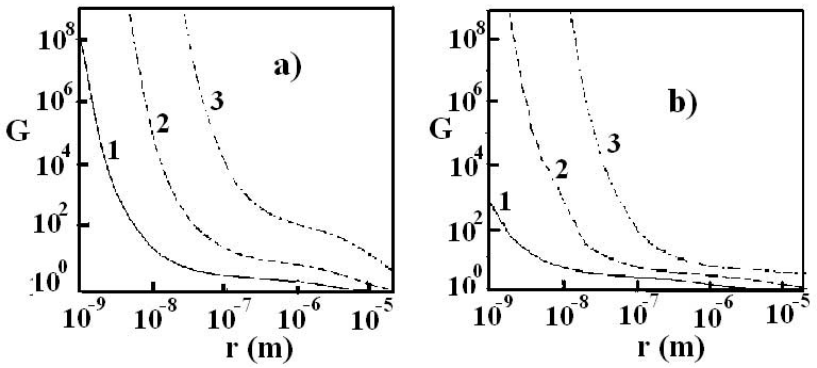


Fig. 3. – The dependence of $G$ upon anode radius for $V_0 = 600$, 300 and 150 V (curves 1, 2 and 3) (a)) and for $P = 0.1$, 0.5 and 3.0 atm (curves 1, 2, and 3) (b)) at other fixed parameters (see the text).

wire should have smooth surface to provide the necessary field. From this point of view NT surfaces containing hexagons of graphite carbon atoms is sufficiently good because they provide smooth electrostatic potentials at distances from NT surface larger than a few maximal distance between the carbon atoms (0.28 nm). SWNT(10,10) has also the advantage of stability and is chemically less reactive. Since the electric field $E(r)$ at the point $r$ near the anode of a cylindrical counter with cathode and anode radii $r_c$ and $r_a$ and applied voltage $V_0$ is given by the expression [37] $|\vec{E}(r)| = V_0/[r \ln(r_c/r_a)]$, the replacement of a metallic wire by much thinner NT for fixed other parameters results in increase of the field everywhere. The multiplication factors, $G$, for the proportional chambers have been calculated in various models in various approximations and compared with available experimental data [38-45]. In the recent works $G$ is evaluated by Monte Carlo simulations [43]. In [44], in particular, it has been shown experimentally and by simulations that the proportional counter resolution is better for thinner anode wires. Unfortunately, there are no theoretical and experimental studies devoted to dependence of $G$ upon the anode radius for very thin wires. For the purposes to obtain such dependences it is enough to estimate $G$ using [41] since as it has been shown experimentally [45] the model [41] provides sufficiently correct estimates.

According to [41]

$$\ln G/(Pr_aS_a) = A(1 + CS_a)\exp[-B/S_a], \tag{2}$$

where $P$ is the gas pressure, $S_a = E_a/P = V_0/[\mathrm{Pr}_a \ln(r_c/r_a)]$ is the ratio of the electric field (at the anode surface) and gas pressure, $A$, $B$ and $C$ are constants [41] for various gas mixtures and pressures.

Figure 3 shows the calculated dependence of $G$ upon the anode radius for a counter with $r_c = 6$ mm filled with xenon for 3 values of applied voltage $V_0$ (fig. 3a) and of gas pressure $P$ (fig. 3b). As it follows from the curves the proportional counters with NT wires provide higher $G$ for lower values of $V_0$ and $P$. Such properties can be important for avoiding the space charge effects in the case of operation with $\alpha$-particles and fission products.

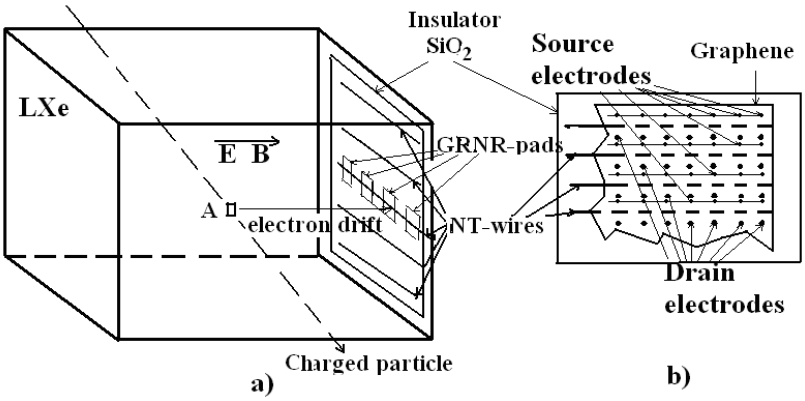


Fig. 4. – The LXeTPC construction and read out planes with NT-wire anodes on the face of a $SiO_2$ insulator (a)) and GRNR or graphene with source (S) and drain (D) electrodes on the other face of a $SiO_2$ insulator (b)).

## 4. – Detector for single particles using graphene

As has been mentioned above, at present there are preliminary results [16-18] on the use of GRNR for constructing miniature dosimeters. The principles of operation of these GR detectors are based on the sensitivity of the electrical conductivity of GRNR to the change of the neighboring electric field due to the collected charges produced by the ionizing radiation in an absorbing layer under the GRFET. In some sense such GR detectors are similar to ionization chambers in which the process of gas amplification is not used. In order to have higher sensitivity it is necessary to increase the number of the collected charge, say, by gas amplification just as in the gas-filled proportional chambers. On the other hand, as has been discussed in sect. **1**, charge amplification up to several hundreds can be obtained only in LXe.

Below we shall only describe the principles of operation and main parameters of a detector (see fig. 4) which as the first proposed xenon chamber [46] is filled with LXe and is based on the ideas of the above-considered NT proportional chambers, NTFET [8,10,11] and GRFET [16-18] detectors (for more details see [47]). The proposed detector allows the detection of the trajectories of charged particles just as the LXe time projection chambers (LXeTPC). In principle, for triggering purposes the proposed LXeTPC can be viewed by photomultipliers (not shown in fig. 4) using the scintillation of LXe as it has been proposed in the work [46] in which the scintillation and ionization charges are used. In the LXeTPC schematically shown in fig. 4 under the influence of the parallel electric, $E$, and magnetic, $B$, fields the electrons from the part A of the particle trajectory drift with a Larmor radius $\sim 1\,\mu$m to readout plane of NT wires providing not high charge amplification, $\sim$100. Charge sensitive amplifiers collect the charges from NTs and measure the $X$-coordinates and energy deposition. The measurement of the variation of the resistivity between the source and drain electrodes of GRNRs (fig. 4a) or a larger GR (fig. 4b) gives the $Y$-coordinates and the change of the electric field behind the 100 nm thick insulator $SiO_2$. This mechanism of sensitivity to the neighboring electric field differs also from that used in the works [16-18] when the arrived ionization electrons without electron multiplication create the change of the electric field near GR. In the case of the

proposed scheme (fig. 4) the number of the arrived electrons is increased by the usual avalanche, however, the electric field near the electron multiplication places will not be increased rapidly since the number of the positive charge of the produced ionized atoms is also increased. After the removal of the fast electrons by the NT anodes, the excess of the slow positive ion charge creates the change of the electric field which is detected by the variation of the resistance between the source and drain contact of GRNR or GR (for more details see [47]).

Without discussing the nanomanipulation and other problems let us assume that the distance between NTs is $\sim 10\,\mu$m, while instead of the $\sim 10 \times 10$ $(\mu\text{m})^2$ GRNR pads shown in fig. 4a, it is better to have larger GR readout planes shown in fig. 4b. The NT anodes are micro fabricated on the inner side of a $\sim 100$ nm thick $SiO_2$, while GRNRs or GR with drain and source electrodes are on the other side of the same $SiO_2$ layer. These source and drain electrodes are fixed by UV lithography. The distances between NT and the source and drain electrodes on GRNRs or GR are equal to $\sim 10\,\mu$m. The source electrodes are connected with each other, while the pulses from each drain electrode go to CCD pixels. As in the usual TPC the $Z$, $Y$ and $X$ coordinates are measured with the help of drift time from the site A to the given NT, by the number of NT and by the number of pad or drain electrode, respectively. The pulse height measurements allow to determine the distribution of energy deposition. As the estimates [47] show, the above-proposed LXeTPC will provide $X$, $Y$ and $Z$ measurement accuracy of the order of $\sim 10\,\mu$m, much better than the existing and proposed similar detectors (see [48-50]) without nanotubes and graphene. Such LXeTPCs can find wide application as advanced detectors for micro-PET.

## 5. – Conclusions

The most difficult problems facing the proposed advanced NT and GR detectors are connected with the facts that it is not possible to see NTs as well as with the necessary accuracies of their microfabricating, aligning and surveying for long term. On the other hand, since in the case NT anodes the electric fields are much higher, and the sensitivity of GR to the variation of neighboring field has not been sudied satisfactorily, it is necessary to develop new theories or models and to carry out experimental tests. The experience of construction of new detectors, such as transition radiation detectors, TPC, etc., shows that the above study is necessary for the required many years of RD works.

REFERENCES

[1] Radushkevich L. V. and Lukyanovich V. M., *Zh. Fiz. Khim.*, **26** (1952) 88.
[2] Iijima S., *Nature*, **354** (1991) 56.
[3] Gevorgian L. A., Ispirian K. A. and Ispirian R. K., *Nucl. Instrum. Methods B*, **145** (1998) 155.
[4] Artru X., Fomin S. P., Ispirian K. A., Shulga N. P. and Zhevago N., *Phys. Rep.*, **412** (2005) 89.
[5] Ispirian K. A. and Ispiryan R. K., *Proc. SPIE*, **6634** (2007) 663419.
[6] Rao F. *et al.*, *Nanotechnology*, **20** (2009) 055501.
[7] Ambrossio M. *et al.*, *Nucl. Instrum. Methods A*, **589** (2008) 398.
[8] Avouris P., *Physics Today*, January (2009) 34.
[9] Tang X. W. *et al.*, *Phys. Med. Biol.*, **50** (2005) 23.
[10] Peng H. B., Hughes M. E. and Golovchenko J. A., *Appl. Phys. Lett.*, **89** (2006) 243502.

[11] Kotani T. *et al.*, *Physica E*, **29** (2005) 505.
[12] Pruitt L., Dissertation, Clemson University, USA (2008).
[13] Kotani T. *et al.*, *Physica E*, **40** (2007) 422.
[14] Geim A. K. and Novoselov K. S., *Science*, **306** (2004) 183.
[15] Geim A. K. and Novoselov K. S., *Nature Mater.*, **6** (2007) 183.
[16] Foxe M. *et al.*, *Detection of Ionizing Radiation Using GRFET*, to be published in *IEEE Trans. NS*, Manuscripts received Febr. 9, 2010.
[17] Childres I. *et al.*, *AIP Conf. Proc.*, **1194** (2009) 140.
[18] Lopez G. *et al.*, presented at *SORMA XII, May 24-27, 2010, Ann Arbor, USA*.
[19] `http://www.pa.msu.edu/cmp/csc/ntproperties`.
[20] Ispirian K. A., Margarian A. T. and Zverev A. M., *Nucl. Instrum. Methods*, **117** (1974) 125.
[21] Landau L. D., *J. Phys. USSR*, **8** (1944) 201.
[22] Blunck O. and Leisegang S., *Z. Phys.*, **128** (1950) 500.
[23] Ispirian K. A. and Margarian A. T., *Nucl. Instrum. Methods B*, **36** (1989) 364.
[24] Zheng L. X. *et al.*, *Nature Mater.*, **3** (2004) 673.
[25] Palacios J. J. *et al.*, *Semicond. Sci. Technol.*, **25** (2010) 033003.
[26] Liu H. *et al.*, *Nanotechnology*, **19** (2008) 445716.
[27] Ispirian K. A., Ispiryan R. K. and Margarian A. T., ArXiv:0908.4830 (2009).
[28] Tenenbaum P. and Shintake Ts., *Annu. Rev. Nucl. Part. Sci.*, **49** (1999) 125; SLAC-PUB 8057.
[29] Bravin E., *Proc. DIPAC 2007*, Venice, Italy, MOO1A02.
[30] Ispirian K. A. *et al.*, *Nucl. Instrum. Methods A*, **336** (1993) 423.
[31] Esin S. K. *et al.*, *Proc. Linac96, Geneva, Switzerland, 1996*, p. 193.
[32] Okotrub A. V. *et al.*, *Pisma Zh. Eksp. Teor. Fiz.*, **81** (2005) 37.
[33] Kolbenstvedt H., *J. Appl. Phys.*, **38** (1967) 4785.
[34] Kolbenstvedt H., *J. Appl. Phys.*, **46** (1975) 2771.
[35] Darbinian S. M. and Ispirian K. A., *Rad. Eff.*, **62** (1982) 207.
[36] Middleman L. M., Ford R. L. and Hofstadter R., *Phys. Rev. A*, **2** (1970) 1429.
[37] Sauli F., Preprint CERN-77-09 (1977).
[38] Rose M. E. and Korff S. A., *Phys. Rev.*, **59** (1941) 850.
[39] Kiser R. W., *Appl. Sci. Res. B*, **8** (1960) 183.
[40] Williams A. and Sara R. I., *Int. J. Appl. Radiat. Isot.*, **13** (1962) 229.
[41] Akande W., *Rev. Sci. Instrum.*, **63** (1992) 4354.
[42] Kocharov G. E. and Korolev G. A., *Izv. Akad. Nauk SSSR*, **27** (1963) 301.
[43] Date H. and Shimozuma M., *Phys. Rev. E*, **64** (2001) 066410.
[44] Rachinhas P. J. B. M. *et al.*, *IEE Trans.*, *NS*, 1 (1995) 90.
[45] Loyola H., Birstein L. and Hevia A., *Radiat. Prot. Dosim.*, **132** (2001) 25.
[46] Ispirian K. A. and Margarian A. T., *Xenon Chambers and Their Applications*, Preprint YerPhI, Scientific Rep. EFI-ME-26 (1972).
[47] Ispirian K. A. *et al.*, *LXe Micro-TPC with NT and GR Readout*, to be published.
[48] Aprile E. and Doke T., *Rev. Mod. Phys.*, **82** (2010) 2053.
[49] Lewellen T. K., *Am. J. Roentgenol.*, **195** (2010) 301.
[50] Retiere F., *Nucl. Instrum. Methods A*, **623** (2010) 591.